Journal of Civil Mechanical Engineering

Volume No. 12

Issue No. 3

September - December 2024

ENRICHED PUBLICATIONS PVT.LTD

JE - 18,Gupta Colony, Khirki Extn,
Malviya Nagar, New Delhi - 110017.
E- Mail: info@enrichedpublication.com
Phone :- +91-8877340707

Journal of Civil Mechanical Engineering

Aims and Scope

The Journal Of Civil Mechanical Engineering publishes original papers within the broad field of civil mechanical engineering it publishes both theoretical and experimental papers which explore or exploit new ideas and techniques in the following areas: structural engineering (structures, machines and mechanical systems), mechanics of materials (elasticity, plasticity, fatigue, fracture mechanics), materials science (metals, composites, ceramics, plastics, wood, concrete, etc., their structures and properties, methods of evaluation) Theoretical papers, practice-oriented papers including case studies, state-of-the-art reviews are all welcomed and encouraged for the advance of science and technology in civil engineering. , All papers are subject to a referee procedure.

Journal of Civil Mechanical Engineering

Journal of Civil Mechanical Engineering

(Volume No. 12, Issue No. 3, September - December 2024)

Contents

Morphometric Analysis of Wadi Qena using SRTM DEM and GIS analysis

Maria Philip
Msc student candidate Geology Department,
South Valley University

A B S T R A C T

In this article, Shuttle Radar Topography Mission (SRTM) Digital Elevation Models (DEMs) data was processed and analyzed using GIS techniques to extract the morphometric parameters of Wadi Qena. This basin subdivided here into 24 sub-basin. The quantitative analysis of the drainage basin revealed values of bifurcation ratio, drainage density, circularity ratio, elongation ratio, form factor, stream frequency and drainage intensity of the studied sub-basins. Analysis and interpretation of the morphometric parameters indicated that few sub- basins vulnerable to flood hazards resulting high runoff in areas of high relief and slope. However, the rest of sub-basins of moderate to low runoff capacity. The quantitative analysis of the studied basin and sub-basins presented meaningful information about the basin characteristics.

Keywords: GIS, Wadi Qena, Morphometric analysis

1. INTRODUCTION

Remotely-sensed digital elevation model (DEM) obtained from SRTM is widely used for analyzing the drainage networks to extract the geomorphic, morphotectonic, morphometric parameters (El Basstawesy et al., 2010; Abdelkareem and El-Baz 2015 a, b; Withanage et al., 2014; Abdalla et al., 2014) and extraction of the tectonic features reflected on topography (Abdelkareem and El-Baz 2015 c, d). Drainage networks extraction also used in lineament extraction and analyses of the drainage basin (Jordan et al., 2005; Simpson 1992), predict the past hydrologic conditions (Strahler 1964; and reconstruction of paleodrainage systems (Abdelkareem et al., 2012 a; Abdelkareem and El-Baz 2016).

Morphometry is defined as the measurement and mathematical processing of the configuration of the earth's surface and of the shape and dimension of its landforms (Clarke, 1966). Morphometric methods, though simple, have been applied for the analysis of area-height relationships, determination of erosion surfaces, slopes, relative relief and terrain characteristics, river basin evaluation, watershed prioritization for soil and water conservation activities in river basins (Kanth, 2012). The use of GIS technique in the morphometric analysis has proven to be a powerful tool in recent years particularly for remote areas with limited access. The aim of the present study is to understand the morphometric characteristics of wadi Qena basin.

2. STUDY AREA

Wadi Qena is located in the Eastern Desert of Egypt that lies between latitudes 26 0 10\ to 28 0 5\ N and longitudes 320 31\ to 320 45\ E ; it`s area is covering about 15746. 5 km2. It represents the major valley of the Nile basin that straddles the eastern Sahara (Abdelkareem and El-Baz 2015 d, Abdelkareem et al., 2012 b. It easily accessible by the asphaltic roads from Qena city along Qena- Safaga road. It also accessible along the Red Sea-Sohag-Asyut road that crossing the Ma'aza Plateau and the Red Sea highlands. However, it is difficult to accessible from north Wadi Qena because of the absence of asphaltic roads and long distance of more than 100 km. It is the region of the most promising areas for future development expansion to the proximity of the River Nile.

Table 1. The calculated parameters and the references of the sub-basins of Wadi Qena

No	Parameter	Symbol/Formula	Reference
1	Stream No. (Nu)	Nu= N1+N2+ +Nn	Horton (1945)
2	Stream length (Lu)	Lu= L1+L2+ +Ln	Strahler (1964)
3	Stream length ratio (R_l)	Rl=Lu/Lu-1	Horton (1945)
4	Bifurcation ratio (Rb)	Rb= Nu/Nu+1	Schumm (1956)
5	Basin Length (Lb) (km)	L_b = the longest in the basin in which are end being the mouth	Gregory and Walling(1973)
6	Area (A) (km)	A	Schumm (1956)
7	Perimeter (P) (km)	P	Schumm (1956)
8	Form factor (Rf)	Rf = A/(Lb)2	Horton (1932)
9	Elongation ratio (Re)	Re = 2?(A/π) / Lb	Schumm (1956)
10	Texture ratio (T)	T = N1/P	Schumm (1965)
11	Circulatory ratio (Rc)	Rc = 4πA/P2	Miller (1953)
12	Stream frequency (Fs)	F_s = ?N_u/A	Horton (1945)
13	Drainage density (Dd)	D_d = ?L_u/A	Horton (1945)

Figure 1. : Location map of wadi Qena basin

4. RESULTS OF DRAINAGE ANALYSIS AND MORPHOMETRIC PARAMETERS

The stream network analysis of entire Wadi Qena basin revealed a 7th order stream, supposing a mature drainage pattern (Abdelkareem and El-Baz 2015 d). Our results reveal that WQ subdivided into 24 sub-basins. The calculated parameters and the references are listed in table 2. The drainage networks analyses of Wadi Qena show dendritic, parallel, and radial drainages on sedimentary rocks, however, the basement shows irregular drainages (Abdelkareem, 2012). The dendritic drainage pattern associated with the limestone plateau that are underlain by homogenous rocks. The major streams at the sedimentary sequence along the main Wadi course are of parallel pattern and the small tributaries join the main stream as trellis that reflects steep slope.

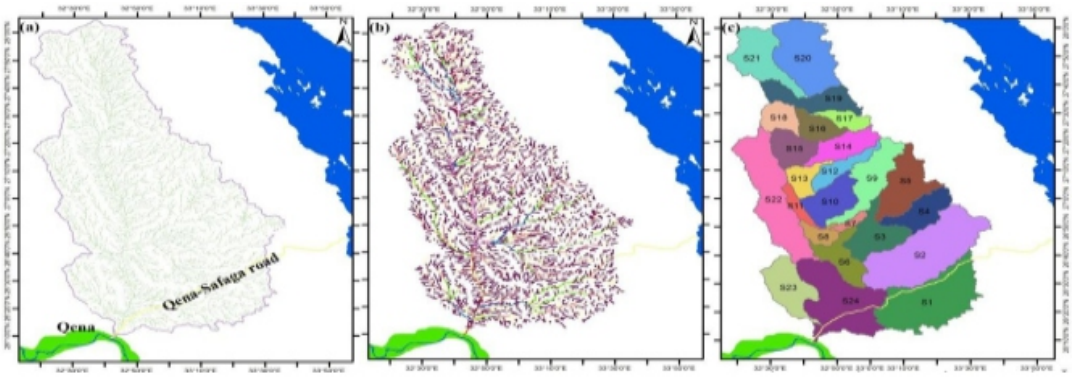

Figure 2. (a) drainage networks; (b) stream order; (c) sub-basins of Wadi Qena

Table 2. Morphometric parameters of Wadi Qena

Basin_NO	U	Nu	Lu	Rb	A	P	Lb	Rf	Re	T	Rc	Fs	Dd
1	6	2240	2324.46	4.45	1469.35	336.6	59.872	0.41	0.722	5.15	0.16	1.52	1.58
2	7	2724	3019.05	3.77	1796.26	324.2	75.275	0.317	0.635	6.51	0.21	1.52	1.68
3	6	848	1036.24	3.5	1871.35	217.4	36.785	1.383	1.327	3.08	0.5	0.45	0.55
4	5	760	737.89	4.96	493.81	183.2	41.708	0.284	0.601	3.23	0.18	1.54	1.49
5	6	1200	1248.87	3.99	775.33	251.3	54.047	0.265	0.581	3.72	0.15	1.55	1.61
6	6	670	807.318	3.62	465.82	215.1	42.003	0.264	0.58	2.47	0.13	1.44	1.73
7	4	153	166.35	4.95	92.24	78.74	22.383	0.184	0.484	1.54	0.19	1.66	1.8
8	5	274	333.12	3.9	195.89	123.6	14.411	0.943	1.096	1.73	0.16	1.4	1.7
9	6	1125	1197.36	3.93	721.67	293.1	66.892	0.161	0.453	2.95	0.11	1.56	1.66
10	6	825	1004.72	3.69	566.56	181.6	25.049	0.903	1.072	3.51	0.22	1.46	1.77
11	5	221	244.432	0.64	157.26	130.9	35.838	0.122	0.395	1.33	0.12	1.41	1.55
12	5	465	535.95	4.43	317.72	188.2	47.306	0.143	0.425	1.99	0.11	1.46	1.69
13	5	495	484.09	4.97	271.88	135.8	20.022	0.678	0.929	2.2	0.19	1.82	1.78
14	6	666	802.17	3.75	467.8	186.2	44.21	0.239	0.552	2.84	0.17	1.42	1.71
15	5	642	766	4.91	439.12	132.1	27.556	0.578	0.858	3.81	0.32	1.46	1.74
16	5	325	610.42	3.99	340.46	139.1	18	1.051	1.157	1.47	0.22	0.95	1.79
17	5	344	381.51	4.4	228.37	125.1	31.471	0.231	0.542	2.16	0.18	1.51	1.67
18	6	453	544.91	3.46	314.24	117.8	26.669	0.442	0.75	0.28	3.07	1.44	1.73
19	6	812	1002.21	3.7	566.63	230.5	17.526	1.845	1.533	2.72	0.13	1.43	1.77
20	6	1674	2196.42	4.24	1187.02	261.7	51.242	0.452	0.759	4.91	0.22	1.41	1.85
21	6	1134	1194.96	3.95	757.9	244.9	56.73	0.235	0.548	3.64	0.16	1.5	1.58
22	6	1969	2120.33	4.48	1377.65	373.4	92.398	0.161	0.453	4.07	0.12	1.43	1.54
23	6	911	986.47	3.83	646.05	210.8	50.317	0.255	0.57	3.37	0.18	1.41	1.53
24	6	1987	2495.28	4.47	1404.01	338.8	54.788	0.468	0.772	4.57	0.15	1.42	1.78

4.1 Bifurcation ratio (Rb)

The Bifurcation ratio (Rb) can be computed by dividing the number of streams in a given order by the number in the next higher order (Schumm 1956). The values of Rb in table 2 are higher in many sub-basins such as S4, S7, S13, S15 that range from 4.482 to 4.973, but the lower in S11 that has 0.641.

4.2 Stream length ratio (Rl)

The Stream length ratio (Rl) is defined as the length of the mainstream in the sub-basin. It`s value ranges from 0.4381 to 0.9512; which the higher value in S7, S11 that reveal elongated basins. However, S3, and S15 are not elongated but almost sub-circular.

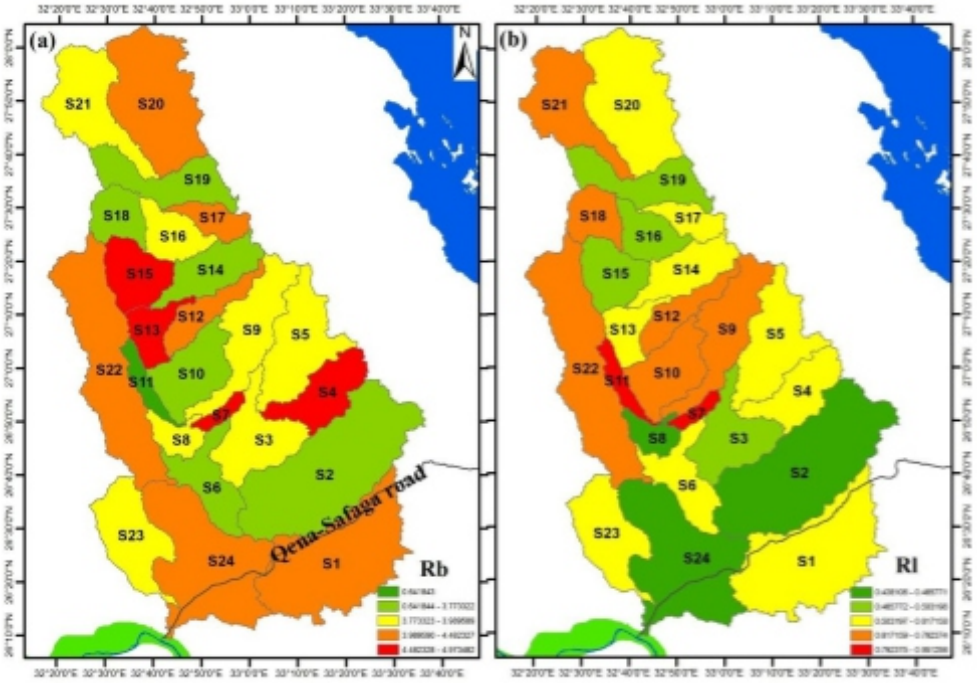

Figure 3. (a) Bifurcation ratio (Rb), and (b) Stream length ratio (Rl)

4.3 Basin length (Lb)

According to Gregorg and Waling (1973), the length of the basin (Lb) is the longest dimension of the basin parallel to the principal drainage line. The length of the studied Wadi Qena sub-basins ranges from 14.41 (S8) to 92.39 km (S 22). However, S2, and S22 area the most elongated basins in length based on computed Lb in table 2.

4.4 Basin area (A)

The total area projected upon a horizontal plane termed "Area" of the basin(Schumm1956). The reform the area (A) of Wadi Qena sub basins ranges from 92.249 (S7) to 1871.351 (S3) km2. Large areas contains several streams rather than the small one, this collect much water to the outlet such as sub-basins S1, S2, S3, S20, S22, and S24.

4.5 Basin perimeter (P)

Perimeter is the length of the boundary of the basin (Schumm (1956). It is measured along the divide between watersheds and may be used as an indicator of watershed size and shape. The perimeter of Wadi Qena sub-basins ranges from 78.743 (S7) to 373.401 (S22) km. We observe a positive relation between of Area and Perimeter, as the sub-basins of high area are of high Perimeter e.g., S2, S22, S24, and S1.

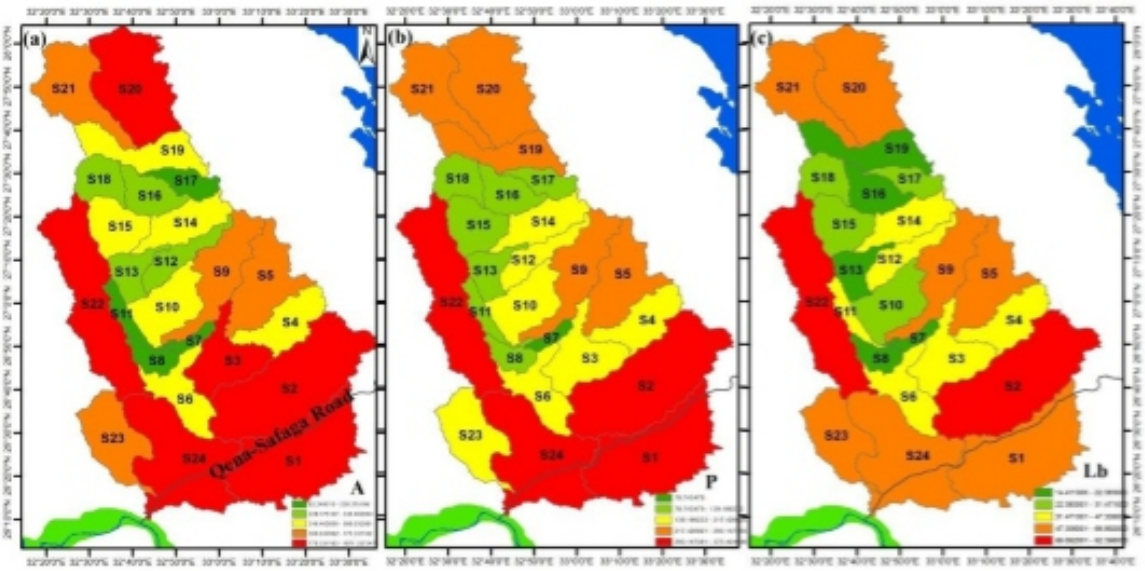

Figure 4. (a) Basin area (A), (b) Basin parameter (p), and (c) Basin length (Lb)

4.6 Elongation ratio(Re)

The elongation ratio (Re) is the ratio between the diameter of the circle of the same area as the drainage basin and the maximum length of the basin (Schumm, 1956). It is a very significant index in the analysis of the basin shape which helps to give an indication about the hydrological character of a drainage basin. The Re ranges from 0.39 (S11) to 1.53 (S19). The Re values (Table 2) are higher in sub-basins S19, S16 but the lower values are in S 11, S12, S19, and S22. Many sub-basins reveal circular shape such as S10, S8, and S3 but the more elongated sub-basins are S11, S22, S9, and S7.

4.7 Form Factor (Rf)

The form factor (Rf) may be defined as the ratio of the area of the basin to the square of basin length (Horton, 1932). The values of form factor would always be less than 0.7584 (perfectly for a circular basin). It is the quantitative expression of drainage basin outline form. The elongated basin with low Rf indicates that the basin has a flatter peak with a longer duration. The Rf range from 0.122 (S11) to 1.84 (S19). The Rf values (Table 2) are higher in sub-basin S19, S3, S16, S8, but the lower values are in S11,S2, S9, S22, S12, S6 that range from 0.1207 to 0.254 .

4.8 Circularity ratios (Rc)

Miller (1953) defined the Circularity Ratio (RC) as the ratio of basin area to the area of a circle having the same circumference as the perimeter of the basin. The author described that the circularity ratios range from 0.4 to 0.5 which indicates strongly elongated and permeable homogenous geologic materials (Withanage et al., 2014). Rc ranges from 0.11 (S9, S12) to 3.07 (S18). Higher the value of Rc S18, S3, and S15 and lower values in S6,S9,S11,S12,S19,S 22.

4.9 Texture ratio (T)

The texture ratio (T) of Schumm (1965) is the ratio of first order population Nu1 to the perimeter (P) of the basin. Based on the computed data in table 4.3 and the distribution of the T values on the studied sub-basins, the T values range from 0.28 to 6.5. This revealing that S1, S2, and S20 of the higher population against the other sub-basins. This allowed to collect much surface water and promoting flood risks.

4.6 Elongation ratio(Re)

The elongation ratio (Re) is the ratio between the diameter of the circle of the same area as the drainage basin and the maximum length of the basin (Schumm, 1956). It is a very significant index in the analysis of the basin shape which helps to give an indication about the hydrological character of a drainage basin. The Re ranges from 0.39 (S11) to 1.53 (S19). The Re values (Table 2) are higher in sub-basins S19, S16 but the lower values are in S 11, S12, S19, and S22. Many sub-basins reveal circular shape such as S10, S8, and S3 but the more elongated sub-basins are S11, S22, S9, and S7.

4.7 Form Factor (Rf)

The form factor (Rf) may be defined as the ratio of the area of the basin to the square of basin length (Horton, 1932). The values of form factor would always be less than 0.7584 (perfectly for a circular basin). It is the quantitative expression of drainage basin outline form. The elongated basin with low Rf indicates that the basin has a flatter peak with a longer duration. The Rf range from 0.122 (S11) to 1.84 (S19). The Rf values (Table 2) are higher in sub-basin S19, S3, S16, S8, but the lower values are in S11,S2, S9, S22, S12, S6 that range from 0.1207 to 0.254 .

4.8 Circularity ratios (Rc)

Miller (1953) defined the Circularity Ratio (RC) as the ratio of basin area to the area of a circle having the same circumference as the perimeter of the basin. The author described that the circularity ratios range from 0.4 to 0.5 which indicates strongly elongated and permeable homogenous geologic materials (Withanage et al., 2014). Rc ranges from 0.11 (S9, S12) to 3.07 (S18). Higher the value of Rc S18, S3, and S15 and lower values in S6,S9,S11,S12,S19,S 22.

4.9 Texture ratio (T)

The texture ratio (T) of Schumm (1965) is the ratio of first order population Nu1 to the perimeter (P) of the basin. Based on the computed data in table 4.3 and the distribution of the T values on the studied sub-basins, the T values range from 0.28 to 6.5. This revealing that S1, S2, and S20 of the higher population against the other sub-basins. This allowed to collect much surface water and promoting flood risks.

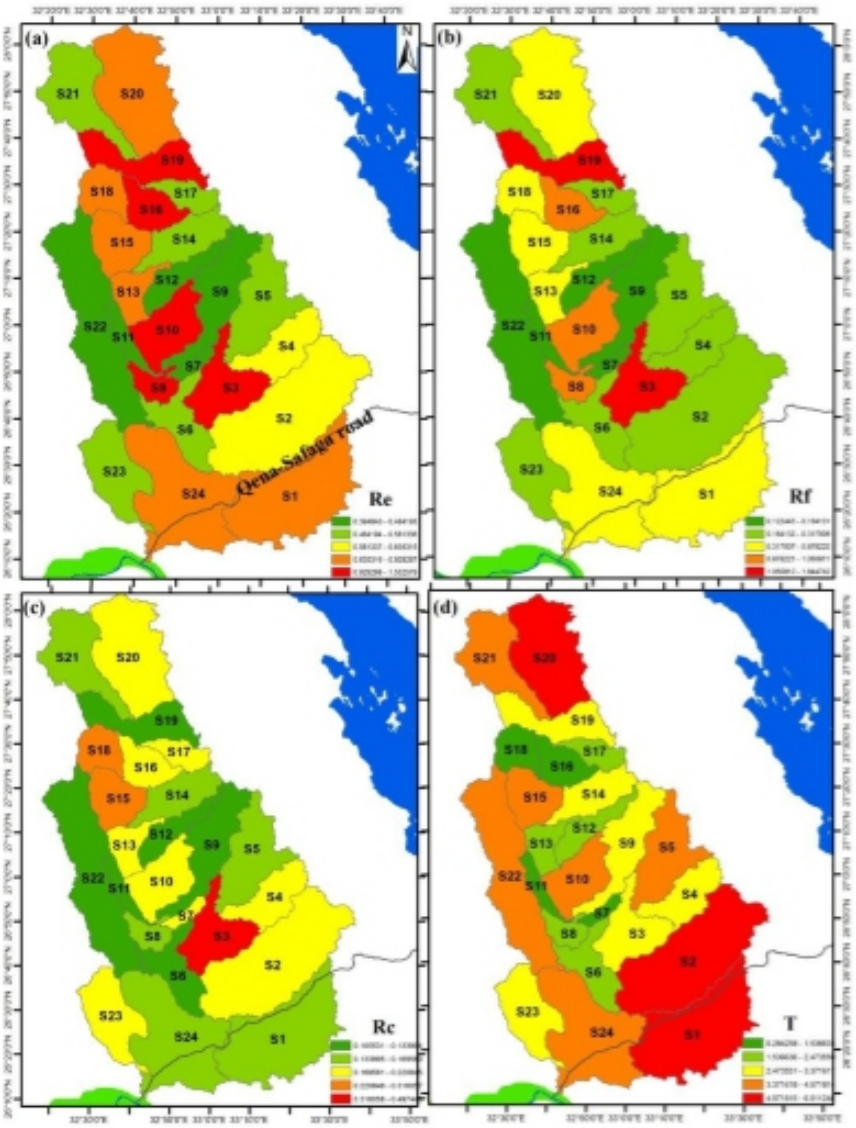

Figure 5. (a) Elongation ratio (Re), (b) Form Factor (Rf), (c) Circularity ratios (Rc), and Texture ratio

4.10 Stream frequency (Fs)

Horton (1932) described the stream frequency (Fs) as the total number of stream segments of all orders per unit area (Table.2). It depends on lithology, structures, infiltration capacity, vegetation cover, relief and amount of rainfall infiltrate to recharge the aquifers. The computed Fs range from 0.45 (S3) to 1,82 (S13). Higher values of Fs reveal fast runoff and the high peak of flood risk such as sub-basins S13, S7.

4.11 Drainage density (Dd)

Horton (1932) defined the drainage density (Dd) as an important indicator of the linear scale of landform elements in stream eroded topography (Horton, 1932). The Dd is defined as the ratio of total length of streams of all orders within the basin to the basin area, which is expressed in terms of km/km2. Dd values may be 1 km per km2 through very permeable rocks; it`s valued range from 0.5537 (S3) to 1.8503km/km2 (S20). Areas of high drainage density relatively high runoff, promoting flood risk. Low Dd reflects erosion-resistant fractures hard rocks and most rainfall infiltrates to recharge the shallow aquifers.

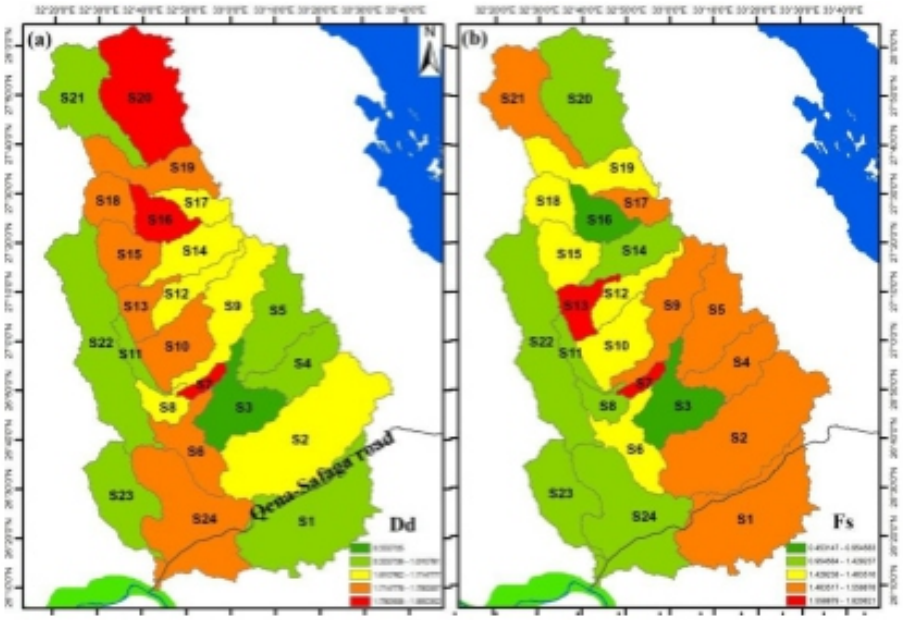

Figure 6. (a) Stream frequency (Fs), and (b) Drainage density (Dd)

6. SUMMARY AND CONCLUSION

Wadi Qena is one of the most important valleys in the Eastern Desert of Egypt. It links the Red Sea, Asyut, Qena, Sohag, and Luxor governorates. It is the region of the most promising areas for development area. It lies between latitudes 26 0 10\ to 28 05\ N and longitudes 320 31\ to 320 45\ E ; it`s covered the area about 15746. 5 km2 .

We computed morphometric analysis for the entire Wadi Qena basin to delineate understand the hydrologic conditions. We subdivided wadi Qena into 24 sub-basins. Several morphometric parameters were mathematically computed using GIS such as bifurcation ratio(Rb), stream length ratio(Rl), basin length(Lb), basin area(A), elongation ratio(Re), form factor(Rf), circularity ratio(Rc), texture ratio(T), stream frequency(Fs), and drainage density (Dd). These parameters spatially distributed to show the higher and lower values of the studied sub-basins.

7. REFERENCES

Abdalla F., El Shamy I., Bamousa A O., Mansour A., Mohamed A., Tahoon M., 2014. Flash floods and groundwater recharge potentials in arid land alluvial basins, southern Red Sea coast, Egypt. International Journal of Geosciences 5: 971-982.

Abdelkareem M, El-Baz F. 2015 a. Regional view of a Trans-African Drainage System. Journal of Advanced Research. Journal of Advanced Research 6: 433–439.

Abdelkareem M, El-Baz F. El-Baz. 2015 b. Analyses of optical images and radar data reveal structural features and predict groundwater accumulations in the central Eastern Desert of Egypt. Arabian Journal of Geosciences (2015) 8:2653–2666.

Abdelkareem M, El-Baz F. Forthcoming 2015 c. Mode of formation of the Nile Gorge in northern Egypt by DEM-SRTM data and GIS analysis. Geol J.

Abdelkareem M, El-Baz F. 2015 d. Evidence of drainage reversal in the NE Sahara revealed by space- borne remote sensing data data. Journal of African Earth Sciences 110, 245-257.

Abdelkareem M, El-Baz F. Forthcoming 2016. Remote sensing of Paleodrainage systems west of the Nile River, Egypt. Journal of Geocarto International.

Abdelkareem M, Ghoneim E, El-Baz F, Askalany M. 2012 a. New insight on paleoriver development in the Nile basin of the eastern Sahara. J Afr Earth Sci. 62:35–40.

Abdelkareem M, El-Baz F, Askalany M, Akawy A, Ghoneim E. 2012 b. Groundwater Prospect Map of Egypt's Qena Valley using Data Fusion. International journal of images and data fusion 3 (2): 169-189.

Abdelkareem M., 2012: (Ph.D) Space data and GIS applications for arid region: Wadi Qena, Egypt.
South Valley University, Egypt; 251 p.

El Basstawesy, M., Faid, A., El Gammal, E., 2010. The Quaternary development of tributary channels to the Nile River at Kom Ombo area, Eastern Desert of Egypt, and their implication for groundwater resources. Hydrological Processes 24, 1856-1865.

Gregory, J.K. and Walling, D.E. (1973) "Drainage basins form and process: A geomorphological approach" Edward Arnold, London, 456pp.

Horton, R.E., (1932). Drainage-basin characteristics. Trans. Am. Geophys. Union, 13, 350-361.

Horton, R. E., (1945). Erosional development of streams and their drainage basins: hydrophysical approach to quantitative morphology. Geological Society of America Bulletin 56, 275-370.

Jordan G., Meijninger B.M.L.., Van Hinsbergen D. J. J.., Meulenkamp J. E., Van Dijk P. M., (2005). Extraction of morphotectonic features from DEMs: Development and applications for study areas in Hungary and NW Greece. International Journal of Applied Earth Observation and Geoinformation 7, 163–182.

Miller, V.C., (1953). A quantitative geomorphic study of drainage basin characteristics in the Clinch
Mountain area, Varginia and Tennessee, Project NR 389042, Tech. Rept. 3., Columbia University, Department of Geology, ONR, Geography Branch, New York.

Schumm, S.A., (1956). The Evolution of drainage systems and slopes in badlands at Perth Amboi, New Jersey. Geological Society of America Bulletins, 67(5).

Simpson, D.W., Anders, M.H., (1992). Tectonics and topography of the Western United States an application of digital mapping. GSA Today 2, 118-121.

Strahler, A.N., (1964). Quantitative Geomorphology of drainage basins and channel networks, Handbook of Applied Hydrology, Ed. Ven Te Chow, 04, 9-76.

Waugh D., 1995. Geography, An Integrated Approach, Nelson, New York, NY, USA,

Withanage, N.S., Dayawansa N.D.K ., and De Silva R.P., 2014. Morphometric Analysis of the Gal Oya River Basin Using Spatial Data Derived from GIS. Tropical Agricultural Research Vol. 26 (1): 175– 188.

An Experimental Investigation on the Fresh Properties of Self-Compacting Concrete Containing Fly Ash, Silica Fume and Lime Powder

Dilraj Singh[*], Harkamaljeet Singh Gil[*], Sarvesh Kumar [**]

[*] Assistant Professor, GNDEC, Ludhiana.

[**] Assistant Professor, PAU, Ludhiana.

ABSTRACT

Self compacting concrete (SCC) is an innovative development of conventional concrete, which requires high binder content to increase its segregation resistance. This paper presents a comparative study on the use of different materials as binder content in SCC and their effects on the workability properties are checked. Different combinations of fly ash, silica- fume and lime powder are used with keeping percentage of OPC constant at 70% of total binder content. Fly ash content is varied from 0 to 30% and silica-fume and lime powder content are varied from 0 to 15%. Water to binder ratio was maintained at 0.41%. Workability tests like V-funnel test, Slump flow test, L-box test and J-Ring test were executed and effects of different combinations of binder content is checked.

1. INTRODUCTION

Self-Compacting Concrete (SCC) is an innovative construction material that does not require vibration for placing and compaction. It is able to flow under its own weight, completely filling formwork and achieving full compaction, even in the presence of congested reinforcement. SCC is compacting itself alone due to its self- weight and is de-aerated almost completely while flowing in the formwork. In structural members with high percentage of reinforcement it fills completely all voids and gaps. SCC flows like “honey” and has nearly a horizontal concrete level after placing. The hardened concrete is dense, homogeneous and has the same engineering properties and durability as traditional vibrated concrete.

Self-compacting concrete extends the possibility of use of various mineral by-products in its manufacturing and with the densification of the matrix, mechanical behavior, as measured by compressive, tensile and shear strength, is increased. On the other hand, the use super- plasticizers or high range water reducers, improves the stiffening, unwanted air entrainment, and flowing ability of the concrete. Practically, all types of structural constructions are possible with this concrete. The use of SCC not only shortens the construction period but also ensures quality and durability of concrete. This non-vibrated concrete allows faster placement and less finishing time, leading to improved productivity.

Khatib (2007) [5] and Liu Maio (2010) [6] studied properties of SCC by replacing cement partially upto 80%. Replacement of cement upto 60% was found to be beneficial and gave strength value around 40 N/mm2. Barbhuiya (2011) [1] studied the utilization of an alternative material, dolomite powder in combination of fly ash, for the production of SCC. It was found that self-compacting concrete can be manufactured using fly ash and dolomite powder with acceptable fresh and hardened properties. Similarly Zhu and Gibbs (2004) [9] studied the fresh properties of SCC using Limestone and Chalk Powders. Vejmelkova et al. (2010) [8] and Khatib and Hibbert (2005) [4] studied the properties of concrete containing Metakaolin and blast furnace slag. Gesoglu et al. (2009) [3] investigated the effects of using binary, ternary, and quaternary cementitious blends of mineral admixtures on the properties of self-compacting concretes and found the optimal mix proportioning.

In this study, an experimental study was done on the fresh properties of SCC containing different combinations of cement, fly ash, silica fume and lime powder. Different combinations were prepared keeping the cement content constant at 70%, varying fly ash contents from 0-30% and varying lime powder and silica fume contents from 0-15%. The fresh properties of the ten different mix combinations were checked and compared.

2. EXPERIMENTAL STUDY

2.1 Materials

Cement: Ordinary Portland cement (OPC) (43 Grade) with specific gravity 3.15 confirming to IS 8112:1989.

Fine aggregate: Sand made of crushed aggregates was used as fine aggregates. Specific gravity of sand was 2.67 and bulk density 1675 Kg/m^3.

Coarse aggregate: Locally available crushed stone aggregates of 12.5 mm nominal maximum size with specific gravity 2.64 and bulk density 1690 Kg/m^3.

Fly ash: Class F Fly ash obtained from Guru Gobind Singh super thermal plant in Ropar with a specific gravity of 2.33.

The chemical properties of Cement and Fly ash are given in the Table 1 and Table 2.

Table 1 Chemical Properties of OPC

S. No.	Constituents	Value (%)	IS 8112-1989 Recommendation (%)
1	Ratio of lime to silica,alumina and iron oxide	0.90%	1.02 (max.) 0.66 (min.)
2	Ratio of Alumina to Iron Oxide	1.58%	0.66 (min.)
3	Insoluble residue	1.10%	2.0 (max.)
4	Magnesia	2.60%	6.0 (max.)
5	Total Sulfur content	1.30%	2.30 (max.)
6	Total loss on ignition	1.20%	5.0 (max.)
7	Total alkali	0.49%	0.6 (max.)
8	Chloride content	0.08%	0.1 (max.)
9. CaO: 61.3%, MgO : 2.60%, SiO_2 : 20.1%, Al_2O_3 : 6.80%, Fe_2O_3 : 4.30%, SO_3 : 1.30%			

Water: Potable water for mixing and curing of concrete specimens was used.

Lime powder: Lime powder having industrial name CARB 2 with specific gravity 2.18.

Silica Fume: Silica Fume named SF88 with specific gravity 2.2.

Super-Plasticizer: Modified Poly-carboxylates type Super-plasticizer of commercial name Sika Viscocrete 20-HE manufactured by Sika. Relative density of Super-Plasticizer was 1.08 at 30°C.

Table 2 Chemical Properties of Fly Ash

S. No.	Constituents	% by weight
1	Loss of ignition	1.2
2	Silica	56.5
3	Ferris oxide	11
4	Magnesia	5.4
5	Alumina (Al_2O_3)	17.7
6	Calcium Oxide	3.2

2.2 Mix design and combinations

The mix proportions of the different materials used are given below in the Table 3. This mix design was prepared after modifications of the mix design got from Su Nan"s (2001) [7] Mix design method.

Table 3 Mix proportions used (Kg/m^3)

Cement	Fly ash	Fine Aggregates	Coarse Aggregates	Water	SP dosage
420	180	882	530	246	4.2

Ten different combinations of binders were prepared keeping the all other parameters constant, as given in Table 4.

Table 4 Combinations of Binders Used (%)

Mix No.	OPC (%)	Fly Ash (%)	Lime powder (%)	Silica Fume (%)
M1	70	30	0	0
M2	70	25	5	0
M3	70	20	10	0
M4	70	15	15	0
M5	70	25	0	5
M6	70	20	0	10
M7	70	15	0	15
M8	70	20	5	5
M9	70	10	10	10
M10	70	0	15	15

3. TESTING THE PROPERTIES OF FRESH CONCRETE

For determining the self-compacting properties; slump flow, T50cm time, J-ring flow, V- funnel flow times and L-box blocking ratio tests were performed [12]. In order to reduce the effect of workability loss on variability of test results, fresh state properties of mixes were determined within a period of 30 min after mixing. The order of testing was as below, respectively.

1. Slump flow test and measurement of T50cm time;
2. J-ring flow test and measurement of difference in height of concrete inside and outside the J-ring;
3. V-funnel flow tests, Time just after filling completely and 5 min T5min;
4. L-box test;

4. RESULTS AND DISCUSSIONS

The results in Table 5 show that the self-compacting concrete was assumed to be having good consistency and workability for all the ten mixes at a constant w/p ratio of 0.41 and at constant SP dosage of 1.0% of weight of cement. All the results were complying the values of the tests specified by EFNARC (2002) [10].

Table 5 Results of Workability Tests

Mix	V-Funnel Time (sec)	Slump Flow dia. (mm)	J-ring (mm)	Slump flow time T500 (sec)	L-box (H2/H1)	V-funnel time after 5 min. (sec)
M1	6.1	780	6	2.9	1	8.9
M2	7.2	740	7	3.3	0.98	10.1
M3	7.9	710	8	3.6	0.96	10.7
M4	8.4	670	9	3.7	0.92	11.2
M5	6.8	690	7	3.3	0.94	8.8
M6	7.8	670	8	3.6	0.93	9.3
M7	8.2	660	10	4	0.89	11.4
M8	7.5	710	8	4.1	0.97	10.1
M9	7.8	690	9	4.3	0.93	10.4
M10	8.9	654	10	4.5	0.9	11.5

The values of the workability tests of M2, M3 and M4 show that when Lime powder was added, the mix becomes dense as compared to the reference mix M1. This was due to the reason that Lime powder is finer than the fly ash and absorbs more water than fly ash. Thus, with the increase in the ratio of lime powder in the mixes, the mix became dense.

The comparison of values of the workability tests of Silica fume mixes M5, M6 and M7 shows the similar trend as in case of lime powder mixes. The values of various workability tests show that the mixes become dense as compared to the reference mix M1, as we increase the Silica Fume content.

The comparison of workability test values of combination mixes with reference mix shows that as we decrease the values percentage of fly ash in the mixes, the mix becomes dense due to addition of both Lime powder and Silica Fume. The mix M10 was found to be most dense mix and least workable mix, because there was no fly ash in the mix and mix was only containing lime powder and Silica Fume in combination.

5. CONCLUSIONS

The following conclusions are drawn from the study.

1. SCC containing the specified replacement levels of different binders as proposed in this investigation was found to be complying with all the workability requirements as per EFNARC (2002). It was found to have good consistency and work ability for all the ten mixes at a constant w/p ratio of 0.41 and constant SP dosage of 1.0% of weight of cement.
2. Comparison of workability test results of different combinations of mixes with the reference mix shows that with decrease in the percentage of fly ash in the mixes, the mix becomes dense and hence less workable.
3. As the percentage of Silica fume is increased the mix becomes denser. Mix M4 was the least workable mix among the Silica Fume mixes. This shows the silica fume mixes require more amount of super-plasticizer content for achieving more workability.
4. Mix M10 was the least workable mix among all the ten mixes, as the fly ash content in the mix M10 was 0 %. Thus the combinations of silica fume and lime powder reduces the workability of the mix.

REFERENCES

1. *Barbhuiya Salim (2011) ,,Effects of fly ash and dolomite powder on the properties of self-compacting concrete" Construction and Building Materials.*
2. *IS: 8112-1989, "Indian Standard 43 grade Ordinary Portland Cement Specification", Bureau of Indian Standards, New Delhi.*
3. *Gesoglu Mehmet, Guneyisi Erhan and Ozbay Erdogan (2009) ,,Properties of self- compacting concretes made with binary, ternary, and quaternary cementitious blends of fly ash, blast furnace slag, and silica fume." Construction and Building Materials 23, 1847–1854.*
4. *Khatib J M and Hibbert J J (2005) ,,Selected engineering properties of concrete incorporating slag and Metakaolin." Construction and Building Materials 19, 460-472.*
5. *Khatib J.M. (2007) ,,Performance of self-compacting concrete containing fly ash". Construction and Building Materials 22, 1963–1971.*
6. *Liu Miao (2010) ,,Self-compacting concrete with different levels of pulverized fuel ash." Construction and Building Materials 24, 1245–1252.*
7. *Su Nan, Su Kung-Chung H and Chai His-Wen. (2001) ,,A simple mix design method for self-compacting concrete". Cement and Concrete Research 31, 1799–1807.*
8. *Vejmelkova Eva, Keppert Martin, Grzeszczyk Stefania, Skalinski Bartłomiej and Robert C erny. (2010). ,,Properties of self-compacting concrete mixtures containing Metakaolin and blast furnace slag". Construction and Building Materials.*
9. *Zhu Wenzhong and Gibbs John C. (2004) ,,Use of different limestone and chalk powders in self-compacting concrete". Cement and Concrete Research 35, 1457– 1462.*
10. *"The European Guidelines for Self Compacting Concrete" EFNARC (2002).*
11. *"Guidelines for testing fresh Self-compacting concrete" (2005).*

Variation of Beam Strength of Steel Gear for Marine Applications

B. Venkatesh[*], V. Kamala [**], A. M. K. Prasad [***]

[*] Associate Professor, MED, Vardhaman College of Engineering, Hyderabad.

[**] Professor, MED, TKR College of Engineering & D G M (Retd.),
BHEL Research & Development, Hyderabad.

[***] Professor, MED, University College of Engineering, Osmania University, Hyderabad.

ABSTRACT

Gears are one of the most critical components in mechanical power transmission system and they are advantage over friction and belt drives. They are positive drives, a feature which most of the machine tools require, since exact speed ratios are essential. Gear design has evolved to a high degree of perfection, the constant pressure to build less expensive, quieter running, lighter weight, reliable, less cost and more powerful machinery has lead to steady change in gear design. The work is to focus on investigating the effects of gear ratio, face width, normal module, speed, pressure angle on beam strength of tooth of steel helical gear for marine applications.

Keywords: Optimization, Helical Gear Design, Modeling, Beam Strength.

1.0 INTRODUCTION:

The motion may be transmitted from one shaft to another shaft with belts, ropes and chains. These drives are mostly used when the two shafts are having long center distance. But if the distance between the two shafts is very small, then gears are used to transmit motion from one shaft to another. In case of belts and ropes, the drive is not positive. There is slip and creep that reduces velocity ratio. But gear drive is a positive and smooth drive, which transmit velocity ratio. Gears are used in many fields and under a wide range of conditions such as in smaller watches and instruments to the heaviest and most powerful machineries like lifting cranes. Gears are most commonly used for power transmission in all the modern devices. They have been used extensively in the high-speed marine engines.

In the present era of sophisticated technology, gear design has evolved to a high degree of perfection. The design and manufacture of precision cut gears, made from materials of high strength, have made it possible to produce gears which are capable of transmitting extremely large loads at extremely high circumferential speeds with very little noise, vibration and other undesirable aspects of gear drives.

Helical gears are the modified form of spur gears, in which all the teeth are cut at a constant angle, known as helix angle, to the axis of the gear, where as in spur gear, teeth are cut parallel to the axis. The following are the requirements that must be met in the design of gear drive, the gear teeth should have

sufficient strength, so that they will not fail under static and dynamic loading during normal running conditions. The gear teeth should have clear characteristics so that their life is satisfactory, the use of space and material should be economical. The alignment of the gears and deflections of the shafts must be considered, because they affect the Performance of the gears. The lubrications of the gears must be satisfactory.

Popular standards are ISO and AGMA. These standards vary in selected approaches as well as models and methods resulting in different design solutions obtained for the same gear under the same set of working conditions. Gear transmissions are widely used in various industries and their efficiency and reliability are critical in the final product performance evaluation. Gear transmissions affect energy consumption during usage, vibration, noise and warranty costs among other factors. These factors are critical in modern competitive, manufacturing, especially in the aviation industry which demands exceptional operations requirements concerning high reliability and strength, low weight and energy consumption, low vibrations and noise. Considering their reliability and efficiency as someof the most important factors, problems of distributions of loads and stresses in the whole gear transmission, particularly in teeth of mating gears, need to be thoroughly analyzed.

DESIGN METHODOLOGY:

The helical gear is design based on AGMA Procedure:

According to Lewis equation Beam Strength of helical gear tooth

$F_b = \sigma_b \cdot b \cdot \pi m_n \cdot y_v$

Number of teeth $Z_v = (Z/\cos^3 \beta)$

Design tooth load $F_{D,} = F_t.K_s.C_v = (F_t.K_s.C_v/v)$

Dynamic load acting on gear according to Buckingham equation $F_d = F_t + \frac{21v(Cb\cos^2\beta + F_t\cos\beta}{21v + \sqrt{Cb\cos^2\beta + F_t}}$

Wear Strength of tooth load $F_w = \frac{d_1 . b . Q . K_w}{Cos^2\beta}$

RESULTS & DISCUSSION

To obtain optimum values of beam strength to achieve low cost of manufacturing for steel gear have been carried out.

Beam Strength- The effect of gear ratio, face width, helix angle and normal module

The effect of beam strength for different input variables are shown in figs. 1(a) – (d). The fig 1(a) shows the relationship between Beam Strength and gear ratio. The helix angle, face width, speed and normal module except gear ratio are kept constant. When gear ratio is increased from 4 to 8, the corresponding Beam Strength remained constant. The fig 1(b) shows the relationship between Beam Strength and Face width. The Helix angles, gear ratio, Speed, normal module except face width are kept constant. When face width is increased from 41 to 49, the corresponding Beam Strength increased from 3320kgf to 3960kgf. The fig 1(c) shows the relationship between Beam Strength and Helix angle. The face width, gear ratio, speed and normal module except Helix angle are kept constant. When helix angle is increased from 15o to 35o, the corresponding Beam Strength remained constant. The fig 1(d) shows the relationship between Beam Strength and Normal module. The face width, gear ratio, speed and Helix angle except Normal module are kept constant. When Normal module is increased from 16mm to 24mm, the corresponding Beam Strength found to increase from 3300kgf to 4890kgf.

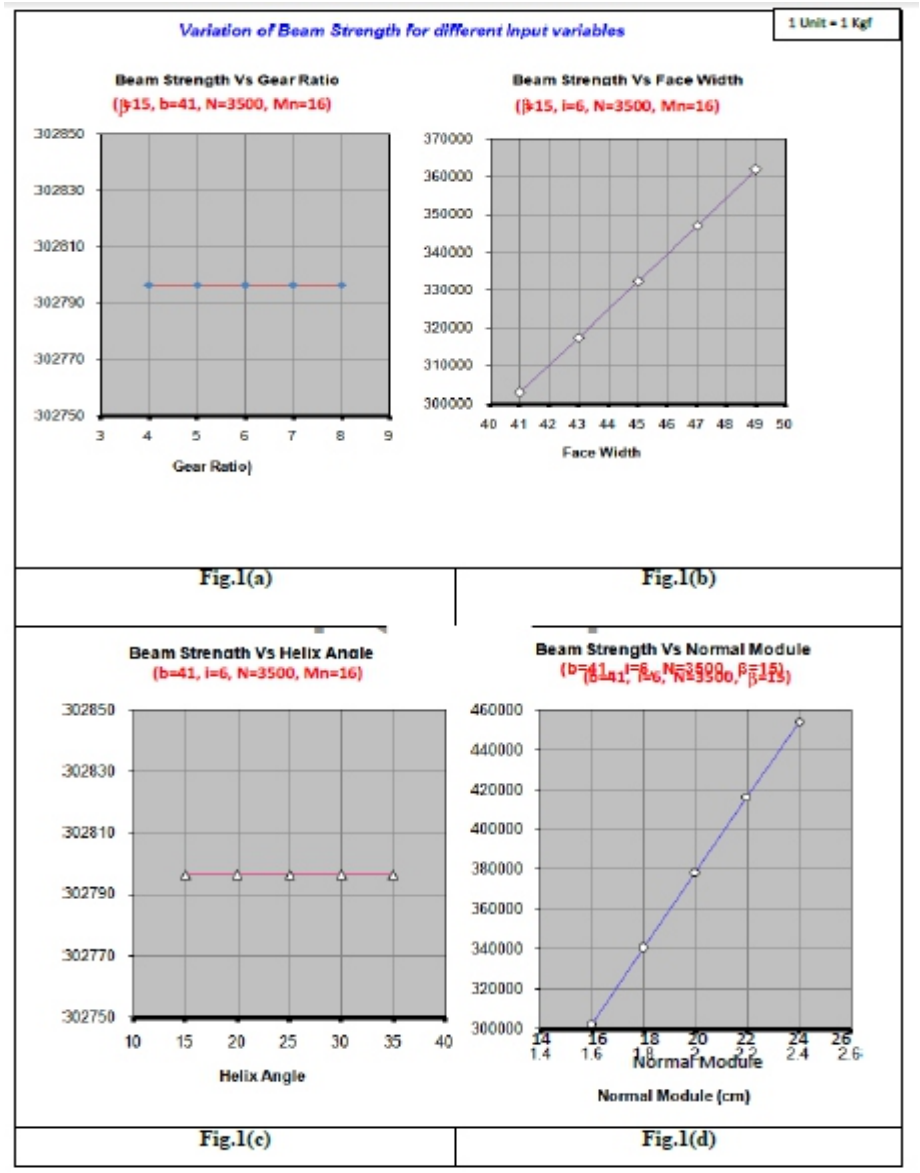

OPTIMUM PARAMETERS FOR MAXIMUM BEAM STRENGTH:

The effect of gear ratio, face width, helix angle, normal module on optimum beam strength is carried out. If the helix angle, face width, speed and normal module except gear ratio are kept constant and gear ratio is increased, the corresponding beam strength remained constant. The helix angles, gear ratio, speed, normal module except face width are kept constant and when face width is increased, the corresponding beam strength increases. The face width 49cm, corresponding to maximum beam strength is taken as constant. The face width, gear ratio, speed and normal module except helix angle are kept constant and helix angle is increased, the corresponding beam strength remained constant. The face width, gear ratio, speed and helix angle except normal module are kept constant and normal module is increased, the corresponding beam strength found to increase. The normal module 24 mm, corresponding to maximum beam strength is taken as constant.

CONCLUSIONS

The study helps to identify the effect of beam strength on the optimum design of helical gears for marine applications. The analysis yielded a beam strength of 361879 kgf for gear ratio of 6, face width of 49, helix angle 150, speed of 3500 rpm and normal module 16. The helical gear parameters that constitute the design are found to be safe from strength and rigidity point of view. Hence 40 N i2 Cr1 Mo28 alloy steel is best suited for marine gear in the high speed applications.

NOMENCLATURE:

σb = Design Bending stress in Kgf/cm² E= Young's modulus in Kgf/cm²

[Mt] = design torque in Kg-cm β = Helix angle in degrees

Fd = Dynamic tooth load in Kgf

Fb = Beam strength of the gear tooth Kgf FD = Design tooth load kgf

mn = Normal Module mm Yv = Lewis Form factor b =Face width in mm

ACKNOWLEDGEMENTS:

The authors are thankful to the managements of their respective Institutions for their encouragement during the course of this work.

REFERENCES

1. Coy, J.J., and Townsend, D.P., 1985,"Gearing"., NASA Reference Publication 1152, AVSCOM Technical Report 84-C-1 5.
2. Alexander L.Kapelevich and Roderick E.Kleiss., Sept/Oct 2002,"Direct Gear Design for Spur and helical Involute Gears"., Gear Technology.
3. Ch.Ramamohana Rao, G.Muthuveerappan., 1993,"Finite element modeling and stress analysis of helical gear Teeth"., Journal of Computers & Structures, Vol. 49, No.6, pp.1095 – 1106.
4. Lazar Chalik, 1996, "Preloaded Gearing for high speed application"., ASME Power transmission & Gearing conference, DE – Vol. 88, pp. 765 – 768.
5. X.Li, G.R.Symmons, Cockerham, 1996,"Optimal design of involute Profile Helical Gears"., Journal of Mechanism and Machine Theory, Vol. 31 No 6, Pp 717-728.
6. Norton, R.L., 1996,"Machine Design: An Integrated Approach"., New Jersey: prentice- Hall Inc.
7. PSG, 2008."Design data," Kalaikathir Achchagam publishers, Coimbatore, India.
8. Barone, S., Borgainil, L., and Forte, P., 2001,"CAD/FEM Procedure for Stress analysis of Un-conventional Gear Applications"., International Journal of Computer Application in Technology, 15, pp.1-11.
9. Alec strokes, 1970, "High performance of gear design"., 10. Darle W. Dudley, 1954," Hand book of practical gear design"., 11. Hwon Y.W., and Bang H., 1999, " The Finite Element Method using MAT LAB"., CRC Press Boka Rotor, USA. 12. http// www.matweb.com

Cam Dynamics and Vibration Control by Detecting Jump

N. S.Ahirrao[*], V. V. Khond[**]

[*] Assistant Professor, Department of Mechanical Engineering, KK Wagh Institute of Engineering Education and Research, Nasik.

[**] Assistant Professor, Department of Mechanical Engineering KK Wagh Institute of Engineering Education and Research, Nasik.

ABSTRACT

Typical industrial cam-follower systems include a force closed cam joint and a follower train containing both substantial mass and stiffness. Providing the cam and follower remain in contact, this is a one degree-of freedom (DOF) system. It becomes a two-DOF system once the cam and follower separate or jump, creating two new natural frequencies. A study was conducted to determine whether imperfections in the cam surface, while the contact force is on the brink of incipient separation, may cause a spontaneous switch to the two-DOF mode and begin vibrations at resonance. A force-closed translating cam-follower train was designed for the investigation. The system is designed to be on the cusp of incipient separation when run. One of the many potential problems with unwanted vibrations in high- speed machinery is the possible introduction of follower jump in a cam-follower mechanism. Jump is a situation where the cam and follower physically separate. When they come back together the impact introduces large forces and thus large stresses, which can cause both vibrations and early failure of the mechanism. This paper will suggest different methods to detect the jump practically with the accuracy. The illustrative experimentation with results will be discussed in this paper.

1. INTRODUCTION:

Many of the journal articles that have been researched focus on a jump phenomena, vibration control, and natural frequencies of cam- follower systems. In a cam follower system, the follower is kept pressed against the cam surface by means of a retaining spring. Due to inertia of the follower, beyond a particular speed, during a part of cam rotation, the follower may loose contact with the cam. This phenomenon is known as cam jump or bounce, which is a type of vibration. This is a transient condition that occurs only with high speed, highly flexible cam follower system. With jump, the cam and the follower separate owing to excessively unbalanced forces exceeding the spring force during the period of negative acceleration. This is undesirable since the fundamental function of the cam follower system, is to constrain and control the follower motion. Also, the life of cam flank surface reduces due to hammering action of follower on cam, hammering noise is also generated. which further results in vibrations of the system.[3,4,5]

2. SOLUTIONS FOR ENSURING CONTACT:

When the cam contact force goes to zero, the cam and follower will separate. Separation occurs at very large negative accelerations of the follower. If there is not a large enough spring force, which is contributed by both the spring constant and the preload, the follower will have the ability to jump from the cam. A large enough spring force and preload must be applied to the cam follower joint at all times to keep them in contact throughout the entire rotation. This large spring force also has the ability to cause problems in a cam follower system. If the spring force is too large, this will increase the contact force, which will induce higher stresses possibly leading to early surface failure of the parts. The motor driving the system will also have to work harder to push the followers through their motions.

The determination of jump characteristics requires that the conventional cam follower system be idealized as a single-degree-of- freedom model, or, for more accurate results, a multi- degree-of-freedom model. In order to detect jump, the acceleration and thus the inertia force of the follower on the closure spring must be calculated. Jump will occur when this inertia force is larger than the spring force. When these two forces are equal then the system is basically on the cusp, balanced and ready for jump to initiate. The contact between the cam and follower can be ensured in two ways: by shape or by force. In the first case, some solutions can be used: cam with channel (groove), cam and counter-cam or cam with slot/notch. These cams ensure the permanent contact between the cam and the cam follower with the help of the cam profiles, but they also lead to design complication and implicitly to manufacturing costs increase, because of the high execution precision implied. In the second case, in order to ensure the contact between the cam and the cam follower, forces or exterior moments can be used, generated with help of spiral or helical springs by gravitation or through additional masses acting over the cam follower, through hydro-pneumatic forces or through centrifugal forces at mechanisms running at high angular velocity. [6,7,8]

3. NATURAL FREQUENCIES AND RESONANCE:

The natural frequency of the follower system is very important to the dynamic behavior of the system. If the operating speed of the machinery in question is close to or is at the natural frequency of the system then that system will go into resonance. Reso nance is a form of free vibration in which the system will vibrate violently, and is extremely harmful to a high-speed machine. Cam mechanisms are driven by the displacement curve or profile of the existing cam; thus the follower motion can be described by a dynamic model or spring mass system under translation-based excitation. Translation based excitation means that the forcing function for the differential equations is the cam displacement function not force acting on the follower. The main rules for the design of high-speed machinery are to use lightweight, strong materials of high modulus of elasticity, to increase the second moment of area and to reduce the

length of the links. In effect, their recommendation can be interpreted as wanting to increase the natural frequencies of the mechanism. [5,7]

4. SOURCES OF VIBRATIONS:

(a) Vibration due to the shape of the follower acceleration curve. An infinite slope or pulse ($da/dt = \infty$) will be seen to be undesirable. With the compression spring loaded follower, this is called "jump".

(b) Vibrations that are a result of separation of the cam and the follower. In positive drive cams with backslash, impact of the roller on the cam is produced, and is called cross over shock. With the spring loaded follower it is due to the "jump" condition.

(c) Vibrations due to surface irregularities, of which they are of many kinds.

(d) Vibrations due to the rate of application of the external load.

(e) Miscellaneous sources as due to cam unbalance. Intelligent practical design o f the cam structure and the body to reduce the offset mass will keep these vibrations to a minimum. Vibrations may be transmitted to the cam surface from the driving mechanism through the frame from such sources as electrical motors, gears and chains.

To reduce the vibrations in the cam follower system, it is suggested that the member from the driver to the follower end be made as rigid as possible.

The conclusion that we can offer for any cam curve at moderate to high speed operation are:

(i) The acceleration maximum value should be kept as small as possible.

(ii) A finite pulse should be maintained at all time, never exceeding the maximum of the cycloidal curve.

(iii) The cycloidal curve is reasonable choice in most cases, giving lower peak forces, vibratory amplitudes, noise and stresses and in general, smoother performance.

The accuracy with which the cam is cut will influence the vibration effects. Play or backlash should be kept to a minimum. Vibration, together with noise and wear, will occur in the dynamical system if it is operated at the speed of its natural frequency. The forces and stresses from vibration are usually superposed on those resulting from normal operation. The operation is affected by the flexibility or elastic deformation of the parts of the system. The parts of the system act as springs of various stiffnesses. The moving parts should be both as rigid and as light as possible. Faulty operation can occur from the difference between the movement at the end of the mechanical chain and the initial movement imposed by the cam. The polydyne cam permits the design of the cam shape to be such that the desired motion will occur at the end of the follower chain. An increase in the pressure angle usually means an

increase in the forces, which must be provided for. The guide for a translating follower may reduce the pressure angle during that portion of the cycle where the forces are the greatest. The mathematical calculations, however, are more involved. A pivoted oscillating fo llower will reduce the side thrust and permit a smaller cam to be used. The spring of a compression system must be strong enough to keep the follower in contact with the cam at all times. This is important in flexible high-speed systems. The follower must not be allowed to jump or leave the cam surface. Sometimes a ramp or small precam is located at the start of the main part of the cam to remove the play and elastic deformation from the system so that the end of the chain will start to move as soon as the main part of the cam begins to act. For light loads and slow speeds, a cam can be composed of sections of circular arcs. Such cams are relatively easy to manufacture and check dimensionally. The acceleration curve, however, has abrupt changes in value. The research that has been presented in this literature review exactly addresses the topic of incipient jump. There has been a significant amount of research conducted on vibration control and dynamic modeling of cam- follower systems. All this information is critical to better understand the problem and to get some idea of how the problem at hand could be addressed.[9,15]

5. EXPERIMENTAL SETUP SPECIFICATIONS:

In this experiment the setup consists of an eccentric cam and a roller follower with a follower spring whose preload can be adjusted. If during the motion at any time the contact force becomes zero then the follower will loose contact with the cam and move independently till the contact is established. This phenomenon is called Jump-off speed. Jump-off speed depends on cam profile, type of follower, spring stiffness and preload, follower mass etc.

The three methods to be introduced for jump detection accurately are

i) Infrared transmitter and receiver circuit

ii) Vibration measurement at bearing housing by FFT Analyzer

iii) Sound level measurement

5.1 SPECIFICATIONS FOR INFRARED TRANSMITTER AND RECEIVER:

Transmitter Section:

Here the IC 555 is the timer IC wired in astable mode. Thus it gives continuous square wave at its pin no.3 whose frequency can be varied by varying the value of resistance. The output is given to the infra-red led which generates IR-light to be transmitted.

Receiver Section:

In this section the 9v supply is converted in to 5v using regulated power supply IC 7805 to drive the IR Receiver module (TSOP-1738) .The IR Rays transmitted is received by the receiver module. This signal is amplified by the power amplifier stage comprising transistors. A reference voltage of 5.1v developed across zener diode, connected to the inverting input. When the voltage level increases beyond the reference voltage, output goes high and this is indicated by glowing the Red LED, as shown in Fig.1.

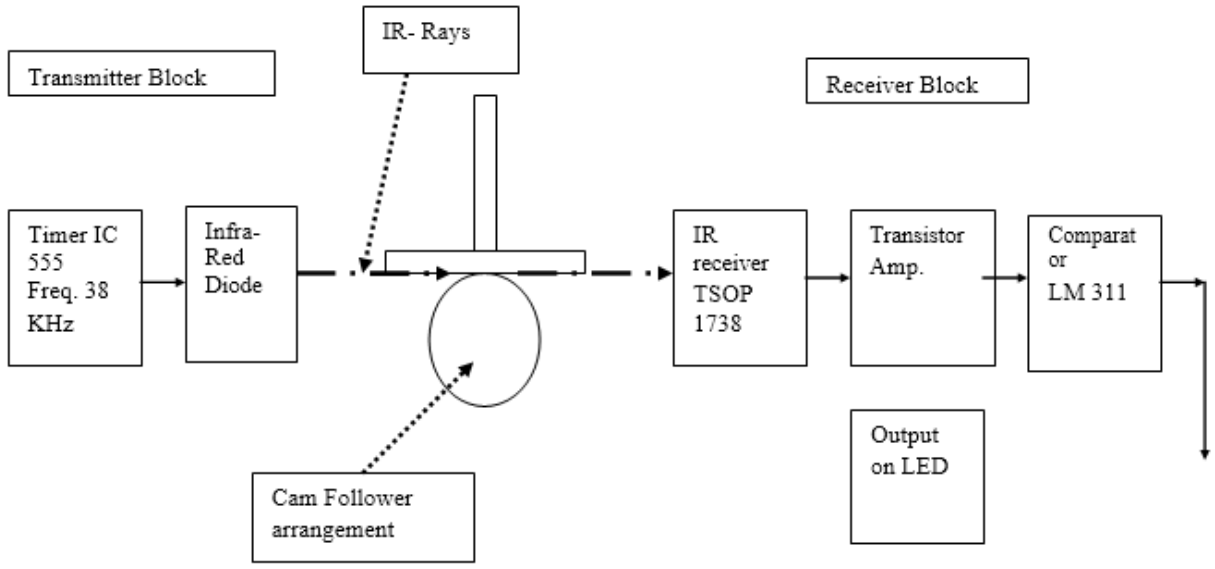

Fig.1: Block diagram of infrared module

5.2 SPECIFICATIONS FOR FFT ANALYZER :

Temperature: 5oC - 50°C

Humidity < 85%

Without strong electric-magnetic field & strong impact

Table 1: Maximum measurement range / frequency range

Parameter	Maximum Measurement Range	Maximum Resolution	Frequency Range
Displacement Peak-Peak value	2 mm	1 micrometer	10 - 500Hz
Velocity RMS value	200mm/s	0.1 mm/s	10 – 1kHz
Acceleration Peak value	250m/s^2	0.1 m/s^2	20 – 10kHz
High Frequency Acceleration Envelope RMS value	20unit	0.1unit	5-1kHz, Demodulated from15-40kHz acceleration

Accuracy:

Frequency response accuracy: ± ±5 %, 10 % for ACC 4. 5 k Hz - 10 k Hz

Non- linearity: ± 5%

Type of sensors: Piezoelectric accelerometer.

5.3 SPECIFICATIONS FOR SOUND LEVEL METER:

Frequency Weighting Network- A & C weighting. Microphone: Electric Condenser Microphone.

Size of Microphone: ½ inch standard size. Operating temperature: 0°C to 50°C.

6. RESULTS:

PROCEDURE: Start rotating the cam and gradually increase the speed till the jump gets detected by any of the methods which could be introduced first of all. Results to be produced are nothing but introducing following methods with remarks and comparisons of these with accuracy.

The preload will be adjusted to maximum and minimum values and the readings can be taken at these conditions.

But for the three methods to be introduced the preload value should not be changed so that the different methods would be accurately assessed and compared.

The Infrared Transmitter and Receiver Circuit will made on and we will measure the sound by sound level meter and vibrations (velocity) by FFT analyzer ,then we get the following sets of readings when jump occurs.

Table 2: Results with three different methods for jump detection:

Sr.No.	Method of Jump Detection	Readings				Remarks	
1	**Jump Detection by Infrared Transmitter and Receiver Circuit**	Preload Levels	RPM at which Jump Occurs		Observations	Preload levels 1 Maximum 2 Minimum	
		1	640	Before the jump occurs	LED off		
		1	658	after the jump occurs	LED on		
		2	545	Before the jump occurs	LED off		
		2	552	after the Jump occurs	LED on		
2	**Jump Detection by Vibration Measurement (Velocity) at Bearing Housing by FFT Analyzer**				Position	Velocity (mm/s)	ISO 2372 Class –I(Less than 15kW) machine A= 0 to0.71 mm/s B =0.71 to 1.8 mm/s C=1.8 to 4.5 mm/s Preload levels 1 Maximum 2 Minimum
				Before the jump occurs	X-axis	0 .56/ 0.71 0.71/	
		1	642		Y-axis	0.84/ 1.8	
		1	660	After the jump occurs	X-axis	1.8/2.66/4.5	
					Y-axis Z-axis	1.8/3.67/4.5	
						1.8/2.45/4.5	
		2	542	Before	X-axis	0.68/0.71	
				the jump occurs	Y-axis Z-axis	0.71/ 1.2/1.8	
						0.71/ 1.3/1.8	
		2	553	After	X-axis	Greater than	
				the jump occurs	Y-axis Z-axis	4.5 mm/s (Not acceptable)	
3	**Jump Detection by Sound Level Measurement**	1	650	When the jump occurs	85 dB		noise for max hold C – weighting
		2	550	When the jump occurs	90 dB		Preload levels 1 Maximum 2 Minimum

7. CONCLUSION WITH DISCUSSION:

Jump will occur when the system is basically on the cusp, balanced and ready for jump to initiate.

Methodologically the Infrared transmitter and receiver circuit provides the visual output but practically it may not be possible always because of space constraints and the kinds of assemblies we would be having.

Vibration measurement at the bearing housings will be more prominent and the results to be seen with permissible range of vibrations and ultimately the jump detection. Finally, to measure the sound level due to jump is also an effective way of detection; only it should be measured at the cusp of separation with the maximum hold position.

The methods are showing significantly the similar range of readings for the speeds at which jump occurs.

We, also should remember the range of vibration levels at the point of jump occurrence and therefore one can not predict the speeds of jump unless and until the levels are set .From vibration readings it is already seen that beyond 4.5 mm/s we should consider there are serious concerns about the vibrations and ultimately total system is in the mode of vibration which indicates the jump occurrence in a system. Our concerns therefore should not be towards speed enhancement which could be possible by selecting proper stiffness and rigidity to the system, but in any circumstances to measure the speed at which jump could get occurred. We hope this paper put enough highlight on the methods of follower jump detections which could be incorporated with respect to any kind of system configurations.

REFERENCES:

1. *J.J. Uicker, J.E. Shigley, J.R.Pennock, "Theory of Machines And Mechanisms", Third Edition, Oxford University Press, 2004, 197-220.*
2. *R.L. Norton "Machine Design- An Integrated Approach." Second Edition, Prentice Hall, New Jersey, 2000, 424-480.*
3. *R.L.Norton "Design Of Machinery", Second Edition, McGraw Hill International Edition, 2002, 587-622.*
4. *J.Harland Billings, "Applied Kinematics", D Van Nostrand Company, Inc, New York,124-139.*
5. *Erik Oberg , Franklin D. Jones and Horton , "Machinery's Handbook" 23rd edition, Industrial Press Inc., New York, 2049-2075.*
6. *Juvinall, Robert C. and Kurt M. Marshek, "Fundamentals of Machine Component*
7. *Design." Third Edition. John Wiley and Sons Inc. New York 2000,199-221.*
8. *R. Militaru, E. Lovasz, "Functional Optimization Of The Cam Mechanisms Using Helical Springs With Variable Geometry", Facta University*
9. *Series: Mechanical Engineering Vol.1, No 10, 2003, pp. 1289 - 1298*
10. *B. Demeulenaere , "Optimal excitation for identification of a cam set-up", Master's thesis, Dept. of Mech. Eng., K.U.Leuven, Leuven, Belgium, 1999.*

11. *S.Graham Kelly, "Fundamentals of Mechanical Vibrations", McGraw Hill International Edition, 2000, 160-180.*
12. *Charles R. Mischke , J.E. Shigley, "Mechanical Engineering Design", Sixth Edition, Tata McGraw Hill , 2004, 587-622.*
13. *M.F.Spotts , T.e.Shoup, "Design Of Machine Elements" , Seventh Edition , Prentice Hall International, Inc, 670-675.*
14. *David H. Myszka , "Machines and Mechanisms,Applied Kinematic Analysis", Third Edition, Pearson Education, 2005, 333-386.*
15. *Thomas G. Beckwith, Roy D.Marangeni, John H. Lienhard," Mechanical Measurements", Fifth Edition, Pearson Education,2003, 730-765.*
16. *G.K. Ananthasuresh, "Design of fully rotatable, roller-crank-driven, cam mechanismsfor arbitrary motion specifications", Mechanism and Machine Theory, 36 (2001) 445-467*
17. *Rao V. Dukkipati, "Vibration Analysis", Narosa Publishing House, New Delhi, 2004, 202-220.*

Structural Dynamic Analysis of Cantilever Beam Structure

Shankar Sehgal*, Harmesh Kumar*
*Faculty, Mechanical Engineering Department, University Institute of Engineering and Technology Punjab University, Chandigarh, India.

ABSTRACT

Structural dynamic analysis is required to understand the vibration related behavior of structures including their eigenvalues, modeshapes and frequency response functions. In this paper, structural dynamic analysis of a cantilever beam structure has been performed. Spatial finite element model of the beam structure is formulated and then analyzed further to produce modal model and response model of the structure. The work is helpful in understanding the dynamic behavior such as extreme versus intermediate positions of modeshapes and point versus transient frequency response functions of the cantilever beam structure.

Keywords: Structural dynamic analysis, Finite element method.

1. INTRODUCTION

Better dynamic testing and analysis tools are becoming the need of the day with the ever increasing demands for better performance and the use of lighter materials in modern day machines and structures. With the modern high performance engines, one can achieve very high speeds in no time, which results in increased vibration and noise problems. Further in the automotive, aircraft and spaceship industries, there is an ever existing demand of attaining better fuel economy; which can be met to a good extent by using thin products as well as with the use of light weight materials such as aluminium and plastics composites instead of the conventionally used heavy weight materials such as steels. Thin and light weight products have lot more tendencies to vibrate than their thick and heavy weight counterparts. Excessive vibrations can even result in pre- mature failure of products, whether it is the suspension of an automobile, wing of an aircraft, the printed-circuit-board (PCB) installed in a spaceship, blades of an air-cooler, or the compact-disc (CD) of a computer etc. On the other hand, consumers of today's world desire for non- vibrating and silent functioning of such products. Thus it becomes very important for engineers to understand the vibration behavior of structures through their dynamic analysis [1]. Dynamic analysis aims at understanding, evaluating and modifying the structural dynamic behavior which involves many terms such as natural frequencies, eigenvalues, eigenvectors, damping ratios, Frequency Response Functions (FRFs) etc.

2. DYNAMIC ANALYSIS OF BEAM STRUCTURE

Dynamic analysis involves the formation of model of the system using Finite Element (FE) method [2]. In this method, a complex continuous region of a structure is discretized into simple geometric shapes

called finite elements such as an axial element, torque element, beam bending element, thin plate bending element, thick plate bending element, etc. Boundary points of such finite elements are called as nodes. The results of structural dynamic analysis can be used for finite element model updating [3]. Dynamic analysis of structures is also the backbone of dynamic design of structures [4, 5]. In this paper the cantilever beam structure, as shown in Fig. 1, has been taken as a case study because of its simplicity and also the ability to represent a variety of mechanical products such as wing of an aircraft, rotor blade of a helicopter, blade of a ceiling fan, needle of a clock, shelve of a civil structure, solar panel of a satellite etc. Dimensions of the cantilever beam structure of MS material are 910 x 50 x 5 mm, having a mass density of 7800 kg/m3. These dimensions have also been reported by Arora et al. but for a fixed- fixed beam structure [6]. The FE model of the beam underconsiderations is developed using 60 beam type elements, each FE having two nodes, thereby resulting in total 61 nodes. At each node, two degrees of freedom are measured, out of which one is the displacement in y-direction and the other is the rotation about z-axis. Both the degrees of freedom of node number 1 are fully constrained. For dynamic analysis purpose, each element is expressed in the form of elemental mass, stiffness and damping matrices. Eq. (1) and (2) represent the elemental mass and stiffness matrices for a beam element.

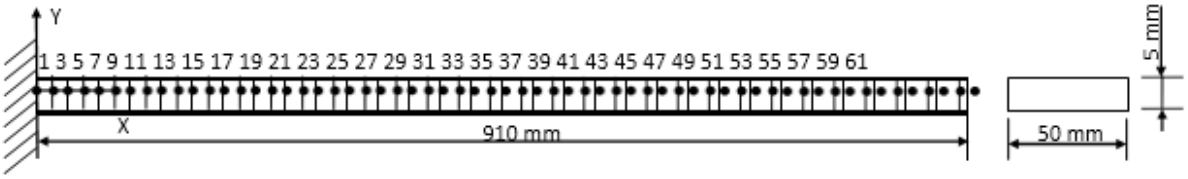

Fig. 1: FE model of a cantilever beam structure

$$[m_e] = \frac{\rho A a}{105}\begin{bmatrix} 78 & 22a & 27 & -13 \\ 22a & 8a^2 & 13a & -6a^2 \\ 27 & 13a & 78 & -22a \\ -13a & -6a^2 & -22a & 8a^2 \end{bmatrix} \quad (1)$$

$$[k_e] = \frac{EI}{2a^3}\begin{bmatrix} 3 & 3a & -3 & 3a \\ 3a & 4a^2 & -3a & 2a^2 \\ -3 & -3a & 3 & -3a \\ 3a & 2a^2 & -3a & 4a^2 \end{bmatrix} \quad (2)$$

Where $m_e, \rho, A, a, k_e,$ and are respectively the element mass matrix, density, area of cross-section of element, half- length of element, element stiffness matrix, Young's modulus of elasticity and moment of inertia of cross-section of beam element. Subsequently, the individual elements are assembled to form their global counterparts, which are also jointly known as system matrices. These system matrices along with certain boundary conditions are used to formulate a set of governing equations, which are then processed on a computer to evaluate dynamic characteristics of the system. Thus it is seen that the dynamic response of the structure depends upon a number of input parameters belonging to material,

structural, finite element and computatio nal categories. In the present research work, the FE model of the beam is processed in Matlab to produce the theoretical dynamic response of the cantilever beam. First six natural frequencies predicted by the FE model are 4.9, 30.9, 86.6, 169.8, 280.7, and 419.4 Hz. The extreme and intermediate positions of different points along the length of beam during first four modes of vibration are also drawn in Fig. 2. The points, having larger displacements from their mean or neutral position, will vibrate at higher average speeds than those points which are displaced to a smaller distance from their mean positions.

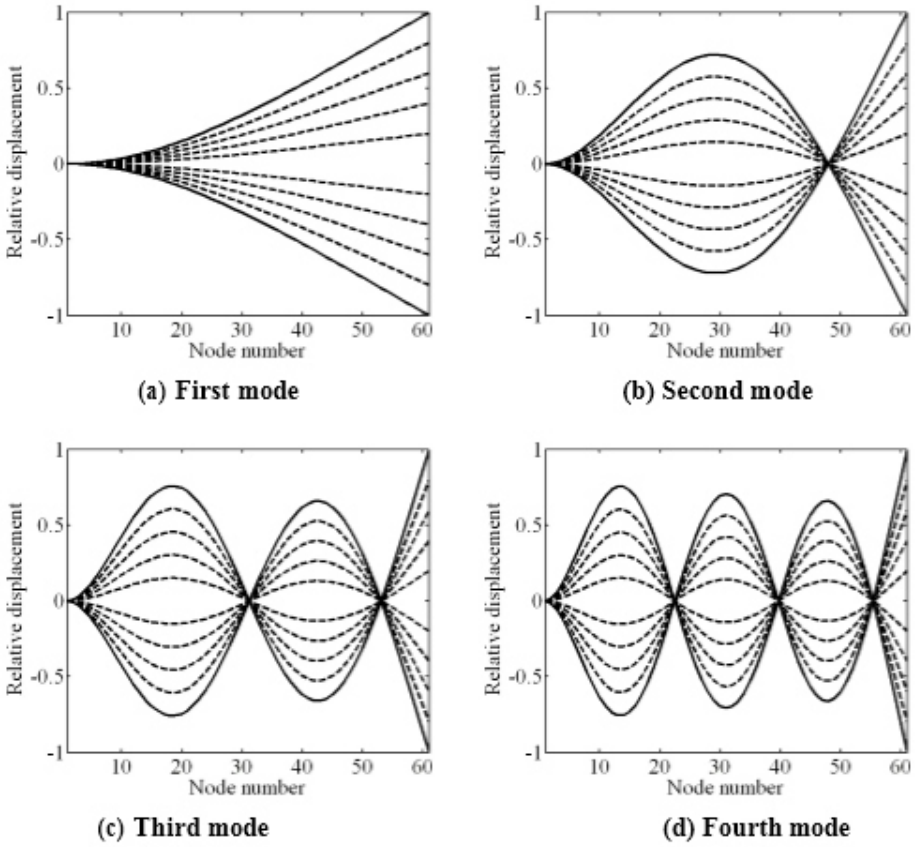

Fig. 2: Extreme and intermediate positions drawn using solid and dashed lines respectively

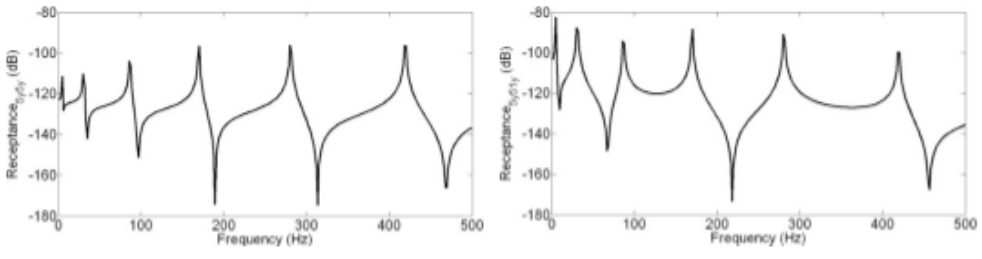

Fig. 3: Frequency response functions of cantilever beam structure

Receptance FRFs obtained during structural dynamic analysis are drawn in Fig. 3. Receptance '5y5y' is drawn in Fig. 3(a), which is a function of displacement signal in 'y' direction at node '5' and force signal in 'y' direction at node '5'. This type of FRF, where displacement and force signals are measured at same

points is called as point FRFs. Another category of FRFs is transient FRFs as drawn in Fig. 3(b), where displacement and force signals are measured at separated nodes. For example, receptance '5y54y' represents a receptance FRF generated using displacement signal at node '5' and force signal at node '54', both in 'y' direction. It is seen that in a point FRF each resonance point (peak) in the curve is followed by an anti-resonance point (valley).

3. CONCLUSION

A cantilever beam structure has been analyzed for its dynamic behavior. Eigenvalues, modeshapes and point as well as transient FRFs have been drawn and analyzed through the application of FE method. The analysis is very useful in the field of structural dynamic modification, dynamic design of structures and finite element model updating. Future efforts will be directed towards use of the results of present research work for finite element model updating of a cantilever beam structure with the help of techniques of design of experiments.

REFERENCES

1. *N. M. M. Maia and J. M. Silva, Theoretical and Experimental Modal Analysis, Research Studies Press Limited, England, 1997.*
2. *M. Petyt, Introduction to Finite Element Vibration Analysis, Cambridge University Press, Cambridge, United Kingdom, 1998.*
3. *M. I. Friswell and J. E. Mottershead, Finite Element Model Updating in Structural Dynamics, Kluwer Academic Publishers, Dordrecht, The Netherlands, 1995.*
4. *R. S. Bais, A. K. Gupta, B. C. Nakra and T. K. kundra, Studies in dynamic design of drilling machine using updated finite element models, Mechanism and Machine Theory, 39, 2004, pp. 1307-1320.*
5. *S. V. Modak, T. K. Kundra and B. C. Nakra, Studies in dynamic design using updated models, Journal of Sound and Vibration, 281, 2005, pp. 943-964.*
6. *V. Arora, S. P. Singh and T. K. Kundra, Finite element model updating with damping identification, Journal of Sound and Vibration, 324, 2009, pp. 1111-1123.*

Instructions for Authors

Essentials for Publishing in this Journal

1 Submitted articles should not have been previously published or be currently under consideration for publication elsewhere.

2 Conference papers may only be submitted if the paper has been completely re-written (taken to mean more than 50%) and the author has cleared any necessary permission with the copyright owner if it has been previously copyrighted.

3 All our articles are refereed through a double-blind process.

4 All authors must declare they have read and agreed to the content of the submitted article and must sign a declaration correspond to the originality of the article.

Submission Process

All articles for this journal must be submitted using our online submissions system. http://enrichedpub.com/ . Please use the Submit Your Article link in the Author Service area.

Manuscript Guidelines

The instructions to authors about the article preparation for publication in the Manuscripts are submitted online, through the e-Ur (Electronic editing) system, developed by **Enriched Publications Pvt. Ltd**. The article should contain the abstract with keywords, introduction, body, conclusion, references and the summary in English language (without heading and subheading enumeration). The article length should not exceed 16 pages of A4 paper format.

Title

The title should be informative. It is in both Journal's and author's best interest to use terms suitable. For indexing and word search. If there are no such terms in the title, the author is strongly advised to add a subtitle. The title should be given in English as well. The titles precede the abstract and the summary in an appropriate language.

Letterhead Title

The letterhead title is given at a top of each page for easier identification of article copies in an Electronic form in particular. It contains the author's surname and first name initial .article title, journal title and collation (year, volume, and issue, first and last page). The journal and article titles can be given in a shortened form.

Author's Name

Full name(s) of author(s) should be used. It is advisable to give the middle initial. Names are given in their original form.

Contact Details

The postal address or the e-mail address of the author (usually of the first one if there are more Authors) is given in the footnote at the bottom of the first page.

Type of Articles

Classification of articles is a duty of the editorial staff and is of special importance. Referees and the members of the editorial staff, or section editors, can propose a category, but the editor-in-chief has the sole responsibility for their classification. Journal articles are classified as follows:

Scientific articles:

1. Original scientific paper (giving the previously unpublished results of the author's own research based on management methods).

2. Survey paper (giving an original, detailed and critical view of a research problem or an area to which the author has made a contribution visible through his self-citation);

3. Short or preliminary communication (original management paper of full format but of a smaller extent or of a preliminary character);

4. Scientific critique or forum (discussion on a particular scientific topic, based exclusively on management argumentation) and commentaries. Exceptionally, in particular areas, a scientific paper in the Journal can be in a form of a monograph or a critical edition of scientific data (historical, archival, lexicographic, bibliographic, data survey, etc.) which were unknown or hardly accessible for scientific research.

Professional articles:

1. Professional paper (contribution offering experience useful for improvement of professional practice but not necessarily based on scientific methods);
2. Informative contribution (editorial, commentary, etc.);
3. Review (of a book, software, case study, scientific event, etc.)

Language

The article should be in English. The grammar and style of the article should be of good quality. The systematized text should be without abbreviations (except standard ones). All measurements must be in SI units. The sequence of formulae is denoted in Arabic numerals in parentheses on the right-hand side.

Abstract and Summary

An abstract is a concise informative presentation of the article content for fast and accurate Evaluation of its relevance. It is both in the Editorial Office's and the author's best interest for an abstract to contain terms often used for indexing and article search. The abstract describes the purpose of the study and the methods, outlines the findings and state the conclusions. A 100- to 250-Word abstract should be placed between the title and the keywords with the body text to follow. Besides an abstract are advised to have a summary in English, at the end of the article, after the Reference list. The summary should be structured and long up to 1/10 of the article length (it is more extensive than the abstract).

Keywords

Keywords are terms or phrases showing adequately the article content for indexing and search purposes. They should be allocated heaving in mind widely accepted international sources (index, dictionary or thesaurus), such as the Web of Science keyword list for science in general. The higher their usage frequency is the better. Up to 10 keywords immediately follow the abstract and the summary, in respective languages.

Acknowledgements

The name and the number of the project or programmed within which the article was realized is given in a separate note at the bottom of the first page together with the name of the institution which financially supported the project or programmed.

Tables and Illustrations

All the captions should be in the original language as well as in English, together with the texts in illustrations if possible. Tables are typed in the same style as the text and are denoted by numerals at the top. Photographs and drawings, placed appropriately in the text, should be clear, precise and suitable for reproduction. Drawings should be created in Word or Corel.

Citation in the Text

Citation in the text must be uniform. When citing references in the text, use the reference number set in square brackets from the Reference list at the end of the article.

Footnotes

Footnotes are given at the bottom of the page with the text they refer to. They can contain less relevant details, additional explanations or used sources (e.g. scientific material, manuals). They cannot replace the cited literature.
The article should be accompanied with a cover letter with the information about the author(s): surname, middle initial, first name, and citizen personal number, rank, title, e-mail address, and affiliation address, home address including municipality, phone number in the office and at home (or a mobile phone number). The cover letter should state the type of the article and tell which illustrations are original and which are not.

Notes: